Articles in PresS. Am J Physiol Lung Cell Mol Physiol (February 18, 2011). doi:10.1152/ajplung.00202.2010

Inflammatory signatures for eosinophilic versus neutrophilic allergic pulmonary inflammation reveal critical regulatory checkpoints

Running title: IMMUNE MEDIATORS IN MODELS OF AIRWAY ALLERGY

Pieter Bogaert[1,2*], Thomas Naessens[1*], Stefaan De Koker[1], Benoit Hennuy[3], Jonathan Hacha[4], Muriel Smet[1], Didier Cataldo[4], Emmanuel Di Valentin[5], Jacques Piette[5],, Kurt G. Tournoy[7], Johan Grooten[1]

[1] Laboratory of Molecular Immunology, Department of Biomedical Molecular Biology, Ghent University, Ghent, Belgium

[2] Department for Molecular Biomedical Research, VIB, Ghent, Belgium

[3] Transcriptomic Unit, GIGA-Research, University of Liège, Liège, Belgium

[4] Laboratory of Biology of tumors and development, GIGA-Research, University of Liège, Liège, Belgium

[5] Laboratory of Fundamental Virology and Immunology, GIGA-Research, University of Liège, Liège, Belgium

[7] Department of Respiratory Medicine, Ghent University Hospital, Ghent, Belgium

[*] P. Bogaert and T. Naessens contributed equally to this work

Corresponding author and address reprints: Dr. Johan Grooten, Laboratory of Molecular Immunology, Department of Biomedical Molecular Biology, Ghent University, Technologiepark 927, B-9052 Ghent, Belgium. E-mail: johan.grooten@ugent.be. Phone: +32 (0)9 33 13 650. Fax: +32 (0)9 33 13 609

Abstract

Contrarily to the Th-2-bias and eosinophil-dominated bronchial inflammation encountered in most asthmatics, other patients may exhibit neutrophil-predominant asthma sub-phenotypes along with Th-1 and Th-17 cells. However, the etiology of many neutrophil-dominated asthma sub-phenotypes remains ill-understood, in part due to a lack of appropriate experimental models. To better understand the distinct immune-pathological features of eosinophilic versus neutrophilic asthma types, we developed an Ovalbumin (OVA)-based mouse model of neutrophil-dominated allergic pulmonary inflammation. Consequently, we probed for particular inflammatory signatures and checkpoints underlying the immune-pathology in this new model as well as in a conventional, eosinophil-dominated asthma model. Briefly, mice were OVA-sensitized using either aluminium hydroxide (alum) or Complete Freund´s (CFA)-adjuvants followed by OVA aerosol challenge. T-cell, granulocyte and inflammatory mediator profiles were determined along with alveolar macrophage genome-wide transcriptome profiling. In contrast to the Th-2-dominated phenotype provoked by alum, OVA/CFA-adjuvant-based sensitization followed by allergen challenge elicited a pulmonary inflammation that was poorly controlled by dexamethasone, and in which Th-1 and Th-17 cells additionally participated. Analysis of the overall pulmonary and alveolar macrophage inflammatory mediator profiles revealed remarkable similarities between both models. Nevertheless, we observed pronounced differences in the IL-12/IFN-γ axis and its control by IL-18 and IL-18 Binding Protein (BP), but also in macrophage arachidonic acid metabolism and expression of T-cell instructive ligands. These differential signatures, superimposed onto a generic inflammatory signature, denote distinctive inflammatory checkpoints potentially involved in orchestrating neutrophil-dominated asthma. **Key words:**

neutrophil-predominant asthma, allergic inflammation, alveolar macrophage, transcriptome, mouse models

List of abbreviations

APC= Antigen Presenting Cells
Alum= Aluminium hydroxide
AM= Alveolar Macrophages
BAL= Broncho-Alveolar Lavage
BP= Binding Protein
CFA= Complete Freund´s (CFA)-Adjuvants
DAMP= Danger Associated Molecular Patterns
DAVID= Database for Annotation, Visualization and Integrated Discovery
DC= Dendritic Cells
Dex= dexamethasone
EASE= Expression Analysis Systematic Explorer
ELISA= Enzyme-Linked Immunosorbent Assay
IL= Interleukin
i.p.= intra-peritoneal
KEGG= Kyoto Encyclopedia of Genes and Genomes
LT= Leukotriene
LX= Lipoxin
HBSS= Hank's Balanced Salt Solution
H&E= Haematoxylin & Eosin
HP= Hypersensitivity Pneumonitis
MMP= Matrix Metalloproteinase
OVA= Ovalbumin
PBS= Phosphate-Buffered Saline
PD-L= Programmed Death-Ligand
PIR= Protein Information Resource
PG= prostaglandin
RT-qPCR= Reverse Transcriptase-quantitative Polymerase Chain Reaction
SPF= Specific Pathogen Free

TCM= Tissue Culture Medium

Th= T-helper cell

Tc= cytotoxic T-cell

Introduction

Predominance of eosinophils in the airway wall and sputum constitutes a major pathological hallmark of persistent mild-to-moderate asthma, commonly defined as a chronic inflammation of the airways mediated by Th-2 cells and provoked in atopic individuals by repeated cycles of allergen inhalation (5, 18, 25). However, asthma is a heterogeneous disease and the emphasis on a Th-2-bias and eosinophilic bronchial inflammation fails to explain clinical observations in many cases in which patients present increased neutrophil cell counts in the airway lumen as a distinguishing trait, especially during acute exacerbations (13, 15, 21, 25). Furthermore, Th-1 cells and cytotoxic T-cells (Tc), bronchiolitis and even alveolitis can often be detected in those patients (5, 9, 10, 18). Recently obtained data also show involvement of Th-17 cells in the patho-physiology of neutrophil-predominant asthma, inducing the release of neutrophil-mobilizing cytokines from airway epithelial cells through IL-17 (1, 5, 9, 17, 28). The etiology of neutrophil-type asthma forms is still ill-understood and precisely those patients with neutrophil-dominated inflammation often present with severe disease that appears resistant to conventional anti-inflammatory glucocorticoid treatments (1, 12, 37). Moreover, experimental research is hampered by the current lack of suitable mouse models that mimic specific features of this condition (14).

Remarkably, several aspects of neutrophilic asthma are prominently found in another type of allergic airway disease, namely hypersensitivity pneumonitis (HP) (16, 33, 49). Similarly to asthma, the HP-pathology is induced by exposure to airborne antigen in sensitized individuals. Th-1, Th-17 and Tc-cells are the main lymphocytic components in HP and were shown to mediate pathology in experimental HP-models (20, 43). Nevertheless, both allergic diseases differ in the nature of their causative agents: asthma-allergens are usually large proteins exerting enzymatic activity, whereas HP-eliciting allergens are often small proteins of microbial origin.

Differences in Danger Associated Molecular Patterns (DAMPs), either intrinsic to the allergen or coinciding at the time of allergen inhalation, are considered as critical in determining the type of ensuing allergic disease (6).

These considerations made us speculate that a neutrophil-dominated allergic airway inflammation reminiscent of common neutrophil-predominant asthma sub-phenotypes could be raised *in vivo* as the result of an 'accidental' Th-1/Th-17-biased sensitization against antigens that intrinsically do not elicit danger signals necessary to sustain this type of response (6). In this study, we show that mice inhaling the model-allergen OVA develop allergic pulmonary inflammation with characteristics of neutrophil-predominant asthma if prior sensitization occurs in the presence of CFA, a potent Th-1/Th-17-skewing adjuvant commonly used in mouse models of HP (6, 20, 41, 43). In addition, we exploited this new model of neutrophilic pulmonary inflammation as well as a conventional model of eosinophilic allergic pulmonary inflammation to seek by comparative expression analysis for distinct inflammatory signatures indicative of regulatory checkpoints controlling neutrophil-dominated asthma-like disease.

Methods

Mouse models and collection of samples

Female, 6-8 weeks-old C57BL/6 mice (Janvier, Le Genest St-Isle, France) were kept under Specific Pathogen Free (SPF)-conditions. Mice were immunized subcutaneously at day 0 with 20 µg of grade V chicken egg OVA (Sigma-Aldrich, St.Louis, MO) in endotoxin-free Phosphate-Buffered Saline (PBS; Lonza, Walkersville, MD), emulsified in 75 µl CFA (Sigma-Aldrich) + 25 µl PBS (OVA/CFA model) or were immunized intra-peritoneally (i. p.) at days 0, 7 and 14 with 20 µg of OVA, adsorbed on 1 mg $Al(OH)_3$ (alum; Sigma-Aldrich) in PBS (OVA/alum model). At day 21 and 22, all mice (≥ 6 mice/group) were exposed to aerosols consisting of 0.1% (OVA/CFA) or 1% (OVA/alum) of grade III OVA (Sigma-Aldrich) in PBS. In experiments where Dex was used, mice received i.p. injections with 0, 1, or 2.5 mg/kg Dex (Sigma-Aldrich) in PBS 3h prior to OVA aerosol. Naïve mice received challenges with PBS alone. In some experiments, immunized but unchallenged mice were included. All experiments were done under conditions specified by law (European Directive and Belgian Royal Decree of November 14, 1993) and reviewed and approved (LA140091/07-035) by the Institutional Ethics Committee on Experimental Animals. Twenty hours after the last OVA challenge, all mice were sacrificed for analysis. Broncho-Alveolar Lavage (BAL) was performed with HBSS (Hank's Balanced Salt Solution, Invitrogen, Carlsbad, CA) supplemented with 10 mM EDTA. Supernatant from the first 0.5 mL BAL fluid was stored at -20°C. After BAL, lungs were removed and put in 4% PFA (left lungs) or kept in Tissue Culture Medium (TCM; Invitrogen) on ice for homogenisation (right lungs) or snap-frozen in liquid nitrogen for total lung lysates.

Cell isolation and flowcytometric/histological analysis of inflammation

Lung CD4 T-cells were isolated from pooled lungs, minced and digested with collagenase (Sigma-Aldrich). After removal of red blood cells, CD4 T-cells were isolated using biotinylated anti-CD4 (Pharmingen) and Dynal magnetic beads (Invitrogen). $CD11c^{high}$/$autofluorescence^{high}$ AM were isolated from pooled BAL cells by flowcytometric sorting using an Altra station (Beckman Coulter, Fullerton, CA). Labeling with anti-CD16/CD32 to block nonspecific binding and with anti-CD11c (Pharmingen) was performed at 4°C. Purity exceeded 95%.

Flowcytometric analyses were performed on a FACSCalibur or LSR-II (BD Biosciences, San Jose, CA). The BAL cellular composition of individual mice was determined by analysis of surface expression of CD3ε, B220, CCR3, I-Ab and CD11c, or CD3ε, CD4, CD11b, CCR3, I-Ab and CD11c (45, 47). Expression of co-stimulatory ligands on alveolar macrophages (AM) or DC was analyzed on pooled BAL cells by surface expression of CD11c and I-Ab in combination with CD40, CD80, CD86, PD-L1 or PD-L2. Lung T-helper cell (Th) phenotypes were determined by analysis of surface expression of CD45, I-Ab, F4/80 and CD4, in combination with expression of IL-17, IL-4 and IFN-γ, or appropriate isotype controls. All antibodies were from Pharmingen (BD, San Diego, CA), except CCR3 (R&D Systems, Abingdon, UK). All labeling was performed at 4°C in the presence of anti-CD16/CD32 to block nonspecific binding. Gating strategies are provided in Suppl. Fig. 2

Pulmonary inflammation was quantified on haematoxylin-eosin (H&E) stained paraformaldehyde-fixed paraffin-embedded lung sections.

In vitro restimulation of lung CD4 T-cells

Pooled lungs were minced and digested with collagenase. After removal of red blood cells, lung cells were seeded in culture medium + 1µg/ml anti-CD3. After 1h, Golgi-Plug (Pharmingen) was added and cells were cultured for another 4h upon which they were harvested for flowcytometric analysis as described above. Cells were first stained for surface markers (CD45, I-Ab, F4/80, CD4), then fixed and permeabilized, and subsequently stained for intracellular cytokines (IL-17, IL-4, IFN-γ).

Measurement of inflammatory mediators in BAL fluid

Inflammatory mediators were measured in the first 0.5 mL fraction of the collected BAL fluid. Cytokines and chemokines were measured using the Bioplex suspension array system (Biorad) according to the manufacturer's instructions, using recombinant cytokine standards (Biorad). MMP-9 and MMP-12 levels were determined by SDS-PAGE western blot analysis, using specific monoclonal antibodies (R&D Systems) and peroxidase-conjugated rabbit-anti-mouse IgG (Dako, Denmark) for detection. Active MMP-9 was analyzed by zymography on a SDS–10% polyacrylamide gel + 1 mg/ml gelatin, detected as a lyses 95 kDa band. Culture medium from HT1080 cells served as internal standard. MMP-12 enzymatic activity was analyzed using the EnzoLyte 490 kit (AnaSpec, San Jose, CA, USA), optimized to detect MMP-12 activity in biological samples using a fluorescence quenched substrate (EDANS/DabcylPlusTM FRET peptide). MMP-12 purified enzyme used as positive control was purchased from Sigma (St Louis, Missouri, USA). Complement C3a levels were determined by Enzyme-Linked ImmunoSorbent Assay (ELISA), using anti-C3a clone I87-1162 (BD Pharmingen) for capture and biotinylated I87-419 clone (BD Pharmingen) for detection. Purified mouse C3a protein (BD Pharmingen) was used as standard.

RT-qPCR analysis

Total RNA was prepared using the Aurum total RNA mini kit (Biorad Hercules, CA). RNA quality was determined spectro-photometrically. For RT-qPCR, cDNA was prepared from 1 µg total RNA using oligo(dT), RNase inhibitor and SuperscriptII reverse transcriptase (all Invitrogen). PCR reactions were performed with the SybrGreen-I qPCR Core kit (Eurogentec, Liège, Belgium) and an iCycler (Biorad) instrument. Data were normalized for the expression levels of housekeeping genes (Ribosomal protein L13a and TATA box binding protein). Amplification specificity was confirmed by evaluation of the melting curves. n-Fold differences between samples were calculated using the $2^{-\Delta\Delta Ct}$ method. The PCR primer pair sequences (Invitrogen) are provided in the Supplementary information.

Transcriptome analysis

RNA integrity was confirmed with the automated electrophoresis Experion System using the RNA StdSens Analysis Kit (Bio-Rad). 4 µg of total RNA, labeled using the GeneChip® Expression 3' Amplification One-Cycle Target Labeling kit (Affymetrix, Santa Clara, CA), was hybridized to Genechip Mouse Genome 430A 2.0 (Affymetrix) according to the manufacturer's instructions. Arrays were scanned with an Affymetrix/Hewlett-Packard GeneChip Scanner 3000 7G (Palo Alto, CA). Data were generated with the MAS 5.0 algorithm included in Genechip Operating Software (GCOS). The naïve condition was set as baseline for pair-wise comparison with OVA-induced experimental conditions. The probe sets were filtered on Signal log ratio (>1 for up regulated and <-1 for down regulated transcripts) and on p-value associated with the

Change status (<0.001 for up regulated probe sets, >0,999 for down regulated probe sets). The complete microarray data set can be consulted in the EBI Array Express Database (http://www.ebi.ac.uk/, accession number E-MEXP-2500).

Statistical analysis

Statistical significance on numbers of cells, cell composition, and mediator levels was determined with the Mann-Whitney U test (2 categorical variables) or Kruskall-Wallis test with post-hoc Bonferroni correction (> 2 categorical variables). Significant p-values were ranked as $p<0.05$ (*), $p<0.01$ (**) and $p<0.001$ (***). Data are represented as mean +/-SE or +/-SD (as indicated in the figures).

Results

1. Immunization with CFA predisposes mice to develop a neutrophilic asthma-like pulmonary inflammation that is poorly controlled by glucocorticoids

To verify to what extent Th-1/Th-17-biased sensitization supports the development of neutrophilic asthma-like inflammation, C57BL/6 mice were systemically immunized against the model antigen OVA in the presence of CFA. Sensitization promoting an eosinophilic asthma-like immunopathology was generated by immunization against OVA in the presence of the Th-2-skewing adjuvant alum. Thereafter, mice from both groups were challenged with nebulized OVA for two consecutive days. This then resulted in a significant cell infiltrate in the BAL fluid compared to naïve mice [Fig.1A].

Flowcytometric analysis of cell surface markers [Fig.1B] and histological analysis of H&E-stained lung tissue sections [Fig.1C] revealed profound differences in the cellular infiltration between OVA/CFA- and OVA/alum-sensitized mice. As expected, the BAL fluid from the well-established OVA/alum model contained mainly eosinophils (± 70%), AM/DC ((± 15%), lymphocytes (± 10%) and fewer neutrophils (< 10%). Histological analysis showed infiltration of eosinophils and monocytic cells almost exclusively around the peribronchiolar and perivascular areas. Contrarily, in the OVA/CFA-sensitized group, we found a substantial infiltration into the broncho-alveolar space of neutrophils, AM/DC and lymphocytes (each ± 30%), and to a lesser extent eosinophils (± 10%) [Fig.1B]. Analysis of lung sections showed a strong infiltration of lymphocytes, monocytic cells and neutrophils around peribronchiolar and perivascular areas, although also a patchy interstitial infiltrate was observed [Fig.1C].

To investigate the responsiveness to anti-inflammatory glucocorticoid treatment, mice from both OVA/alum and OVA/CFA immunized groups received i.p. injections of Dex prior to OVA inhalation, and BAL cellular infiltration was examined after 2 OVA challenges [Fig. 2, Suppl. Fig. 2A]. In the OVA/alum model, pretreatment with either 1mg/kg or 2.5mg/kg Dex showed a potent reduction in infiltrated eosinophils, neutrophils, recruited ($CD11b^{+}$ $autofluo^{med}$) AM, DC, and CD4 T-cells. In the OVA/CFA model however, 1mg/kg Dex had no effect on cellular inflammation while 2.5mg/kg Dex reduced the number of DC and CD4 T cells and to a lesser extent of eosinophils, but had no effect on the neutrophil cell count. Thus, using either alum or CFA as adjuvants predisposes mice to develop divergent types of pulmonary inflammation that are in line with many inflammatory aspects of respectively human eosinophilic and neutrophilic asthma types.

2. Lung CD4 T-cell phenotypes

We characterized the local Th-phenotype generated in the OVA/CFA- and OVA/alum-groups by performing RT-qPCR on magnetically purified lung tissue CD4 T-cells [Fig.3A] and by flowcytometric phenotyping of interstitial lung lymphocytes after *in vitro* culture with α-CD3 [Fig. 3B, Suppl. Fig. 2B]. mRNA expression of the Th-1 transcription factor, T-bet, was induced solely in the OVA/CFA model, while its Th-2 counterpart, GATA-3, was slightly induced in OVA/alum- and OVA/CFA-mice. mRNA expression of the Th-17 transcription factor, ROR-γt, was also induced in both models albeit more prominently in OVA/CFA-mice. Quantification of *in vitro* reactivated lung tissue $CD4^{+}$ T-cells confirmed this differential Th-phenotype: larger IFN-γ^{+} IL-17^{-} Th-1 and IL-17^{+} Th-17 $CD4^{+}$ T cell populations in the lung leukocytes from

OVA/CFA compared to OVA/alum, and similar levels in both models of IL-4^+ Th-2 $CD4^+$ T cell population.

We also quantified the absolute levels of T-cell-derived or -associated cytokines in the BAL fluid by a multiplexed antibody assay [Fig.3C]. Reflecting the higher numbers of BAL T-cells, IL-2 levels were increased in the OVA/CFA-group. A robust increase in IFN-γ levels, and significantly higher presence of IL-12p40 in OVA/CFA-mice compared to OVA/alum-mice further confirmed the Th-1-component in the OVA/CFA-model. Importantly, also the levels of Th-2 cytokines (IL-4, IL-13 and IL-5) were increased in OVA/CFA, with only IL-5 levels being significantly higher in the OVA/alum group. The dramatically increased IL-17 levels in the OVA/CFA-group then confirmed the presence of Th-17 cells in this model. Finally, IL-10 levels remained unchanged in either group.

3. Innate inflammatory mediator signatures

We verified to what extent the differential T-cell polarization in OVA/CFA- versus OVA/alum-conditions reflected at the local inflammatory mediator level. First, we performed RT-qPCR on total lung mRNA [Fig.4A]. Reflecting the cellular environment, mRNA expression of Th-1-chemoattractant (CXCL10) was induced solely in the OVA/CFA-condition, whereas the induction of Th-2-and eosinophil-recruiting chemokine (CCL11) was observed only in the OVA/alum-group. However, expression of two functionally similar chemokines, Th-1-chemoattractant CXCL9 and Th-2/eosinophil-recruiting CCL9, were induced in both conditions and only showed quantitative differences between both groups.

Next, BAL fluid levels of pro-inflammatory cytokines (IL-1β, IL-6 and TNF-α) and chemokines (CXCL1/KC, CCL2/MCP-1, CCL3/MIP-1α, CCL4/MIP-1β and CCL5/RANTES) were analyzed by a multiplexed antibody assay [Fig.4B]. This revealed merely quantitative differences in inflammatory mediator expression between both groups. Of the cytokines and chemokines analyzed, only TNF-α was not induced, whereas the levels of IL-1β, IL-6 and monocyte/lymphocyte-attracting chemokines CCL2, CCL3, CCL4 and CCL5 were elevated in both groups. Surprisingly, also the levels of the neutrophil chemoattractant, CXCL1, were elevated in both groups to a similar extent. Yet, IL-1β, IL-6, CCL4 and CCL5 levels were more prominent in the OVA/CFA-mice.

Next to cytokines and chemokines, we also analyzed the expression levels of additional inflammatory mediators. The matrix metalloproteinases, MMP-9 and MMP-12, are thought to play detrimental roles in asthma. In line herewith, we observed increased levels of total or processed MMP-9 and MMP-12 levels in OVA/alum mice but also in the OVA/CFA model [Fig.4C]. Finally, as complement C3a has also been implicated in acute allergic airway inflammation, we examined C3a levels in the BAL fluid by ELISA [Fig.4D]. Again, C3a levels were elevated in both models, but more prominently so in OVA/CFA-mice. These results show that the innate inflammatory mediator signature only partially reflects the differential cellular inflammation in the models, with the OVA/CFA-model showing more biomarkers (IL-1β, IL-6, C3a) associated with neutrophil-predominant asthma.

4. Genome-wide transcriptome profiling of AM

AM are long-lived cells residing in the broncho-alveolar cavities that are amongst the first cells to encounter inhaled particles and initiate immune responses, and are a common denominator in the

BAL immune cell composition of both eosinophil- and neutrophil-dominated asthma. To identify (anti-)inflammatory signatures differentially induced by the inflammatory micro-environment in AM from neutrophil-dominated versus eosinophil-dominated pulmonary inflammation, we performed genome-wide transcriptome profiling of flowcytometric purified $CD11c^{high}$ $autofluorescence^{high}$ AM. As shown in Figure 5, both OVA/CFA- and OVA/alum-groups exhibited robust changes in the AM transcriptome with over 2800 genes differentially expressed in each condition compared to naive AM, a large majority of which was upregulated. Strikingly, around 60% of those genes had a concurrent expression pattern, defined as >2-fold up-or downregulated in both conditions. Functional clustering of the commonly upregulated gene set using online 'Database for Annotation, Visualization and Integrated Discovery' (DAVID) bioinformatics resources (19) and the **'**Kyoto Encyclopedia of Genes and Genomes' **(**KEGG) and 'Protein Information Resource' (PIR) databases, identified mainly inflammation-related biological themes, such as cytokine-cytokine receptor interaction, chemotaxis, MHC-II-mediated antigen presentation, JAK-STAT signaling and Toll-Like Receptor signaling. Other gene clusters (Type-I Diabetes Mellitus, cell adhesion molecules) also comprised genes involved in inflammatory signaling and transendothelial migration of inflammatory cells. As apparent from Figure 4, genes induced exclusively in the OVA/CFA-condition displayed an overrepresentation of immune effector functions, which was absent in genes induced exclusively in the OVA/alum-group. In the down-regulated gene sets, no inflammation-related biological themes were found [Fig.5].

6. Generic and condition-specific immune effector gene signatures in AM

The above clustering analysis of differentially expressed AM genes does not take into account quantitative differences in gene expression levels. Therefore, we selected for further analysis an immune effector gene set consisting of chemokines, cytokines, growth factors, genes involved in arachidonic acid metabolism, and genes involved in antigen processing and presentation. Genes having an expression pattern not more than 2-fold different between OVA/CFA and OVA/alum versus naïve were assigned to the generic signature. Genes showing 2-fold to 5-fold differences in expression between the respective inflammatory conditions versus naïve were assigned to the condition-biased signature. Finally, genes over 5-fold differentially expressed between the inflammatory models were assigned to the condition-specific signature. The expression levels of selected genes were further tested by RT-qPCR for confirmation in an independent repeat experiment. The results of this refined transcriptome analysis are shown in Figure 6 and discussed in the ensuing paragraphs.

7. Inflammatory mediator differentials

The majority of differentially expressed (versus naïve) chemo- and cytokines and growth factors showed mRNA levels that were identical or similar in OVA/CFA- and OVA/alum-conditions [Fig.6A-B], indicating that AM are dedicated to establishing a general pro-inflammatory environment and recruiting other leukocytes in both conditions. Importantly, a much smaller condition-specific gene set supplemented this generic gene signature. In line with our previous results, we found elevated expression of CXCL9, CXCL10 and CCL5 to be part of the OVA/CFA-specific gene signature [Fig.6A]. Conversely, the Th-2-/eosinophil-attracting chemokines CCL22 and CCL24 but also the neutrophil/monocyte-attracting CXCL7 were part of the OVA/alum-specific gene signature. Moreover, we found evidence for immune-modulatory

functions of AM. Thus, whereas expression of IL-12b, promoting Th-1 function, was generically increased, IL-18 expression, a potent IFN-γ inducing factor acting synergistically with IL-12, was repressed [Fig.6B]. Repression of IL-18 activity may be even more pronounced in the OVA/CFA-condition, as suggested by the OVA/CFA-specific expression of IL-18BP, a soluble IL-18 scavenger. IL18-BP expression may be induced by an endogenous IFN-γ regulated feedback loop, present only in the OVA/CFA-condition [Fig.6B].

Interestingly, we observed a condition-specific dichotomy in the expression of arachidonic acid-metabolizing enzymes [Fig.6C]. Arachidonic acid can be metabolized into pro- or anti-inflammatory eicosanoids. Expression of the pro-inflammatory leukotriene(LT)-synthesizing enzymes, *Alox5*, *Lta4h* and *Ltc4s,* was generically repressed. Instead, it appears that the main eicosanoids produced in OVA/CFA-AM are anti-inflammatory prostaglandin(PG)E_2 and I_2 through *Ptgs2*, encoding COX2. Conversely, in OVA/alum-AM, expression of *Ptgs1,* encoding COX1, is induced along with a concurrent strong induction of *Alox15,* suggesting a shift towards anti-inflammatory Lipoxin (LX) synthesis.

8. Antigen processing and presentation differentials

Transcriptome analysis suggested that AM gained increased capacities to interact with T-cells and present antigen [Fig.6D]. mRNA expression of CD40, which activates T-cells through binding of CD40 ligand, and of ICAM1, which ligates T-cells through LFA-1, were generically induced. Increased input of MHC-II molecules into antigen-processing endosomes is suggested by induced mRNA expression of MHC-II transcription factor (*C2ta*), CD74 invariable chain (*Ii*), I-A α-and β-chains (*H2-Aa*, *H2-Ab1*), and I-E α-chain (*H2-Eb1*). Although part of the generic gene signature, these genes were invariable higher expressed in the OVA/CFA than in the

OVA/alum condition. The OVA/CFA-induced expression of peptide editors (*H2-Dmb1, H2-Dmb2*) and their inhibitor (*H2-Oa*) are then indicative of a broader range of peptides presented in this condition. Notably, although expression of the MHC-I common light chain (*B2m*), TAP (*Tap1*) and TAP binding peptide transporter (*Tabp*) was generically increased, expression of classical MHC-Ia (*H2-K1*) and non-classical MHC-Ib (*H2-M3*, *Qa-1*, *Qa-2*) genes was biased towards the OVA/CFA-condition. Combined, these data indicate that AM-mediated antigen presentation to CD4 and certainly to CD8 T-cells may be more effective in OVA/CFA-AM than in OVA/alum-AM. The stimulatory versus inhibitory outcome of antigen presentation depends on accompanying co-stimulatory signals. Co-stimulatory ICOSL mRNA expression was repressed in both conditions whereas CD86 (but not CD80) expression was increased. Yet, also co-inhibitory *Pdcd1lg2* (encoding for PD-L2) expression was increased in both conditions and further supplemented specifically in the OVA/CFA-condition with elevated levels of co-inhibitory *Cd274* mRNA (encoding for PD-L1).

9. *Expression of co-stimulatory molecules on AM and DC*

To confirm these findings at the protein level, we performed flowcytometric analysis of selected surface markers on CD11c^{high}autofluorescence$^{med/high}$ AM as well as CD11c^{high}autofluorescence^{low} DC [Fig.7A-B]. In agreement with the transcriptome analysis, we observed moderately elevated surface levels of MHC-II on OVA/alum-AM, and strongly elevated levels on OVA/CFA-AM [Fig.7C]. Furthermore, a fraction of these MHC-II^{high} AM also was CD40^{high}. Analysis of co-stimulatory CD80 and CD86 as well as co-inhibitory PD-L1 and PD-L2 confirmed the findings made at the transcriptome level: in the OVA/CFA-condition, a larger fraction of AM were MHC-II^{high}CD86^{high} and only few CD80^{high}AM were observed

[Fig.7D-E]. Both conditions also showed elevated levels of the co-inhibitory PD-Ls, with PD-L1 elevated mainly in OVA/CFA-AM and PD-L2 mainly in OVA/alum-AM [Fig.7F-G]. Furthermore, in OVA/CFA-AM, expression of PD-L1 coincided with MHC-II expression, indicating that especially in this model AM exert a T-cell restraining function.

Analysis of alveolar DC showed, as expected, a majority of the cells to be MHC-II^{high} CD40^{high} in both OVA/CFA-and OVA/alum-conditions [Fig.7C]. Co-stimulatory CD86 expression was more pronounced in DC than in AM, especially in the OVA/CFA-model [Fig.7E]. Nonetheless, we also observed elevated levels of co-inhibitory PD-L1 and PD-L2, coinciding with elevated MHC-II levels [Fig.7F-G].

Discussion

In this study we addressed the issue of whether mouse models of neutrophil-dominated allergic pulmonary and bronchial inflammation could be developed suitable to effectively study the cellular and molecular pathways underlying such conditions. In humans, neutrophil-predominant asthma forms display some undeniable parallels with HP: neutrophilic infiltration, presence of Th-1, Th-17, and Tc cells, and alveolitis (1, 5, 10, 13-18, 21, 25, 28). A classical protocol to predispose mice for HP consists of immunization against the actinomycete *Saccharopolyspora rectivergula* in the presence of CFA as Th-1/Th-17-inducing immunogenic co-factor (41). Conversely, mice become predisposed to develop features of eosinophil-predominant asthma by systemic sensitization with OVA in the presence of the Th-2-skewing adjuvant alum (14). We here combined these protocols by sensitizing mice against OVA in the presence of CFA. Following OVA inhalation, the resulting pulmonary inflammation featured several cellular and

molecular characteristics of neutrophil-predominant asthma: infiltration of lymphocytes, neutrophils and macrophages, and polarization of local CD4 T-cells towards Th-1 and Th-17, similar to clinical findings (1, 5, 9, 10, 13-15, 28, 42). Importantly, we also observed eosinophilic infiltration and evidence of a Th-2-cell component.

In general, asthmatics with neutrophil- and Th-17-dominated inflammation tend to display an increased severity of disease, and both murine and clinical data suggest a relation with steroid resistance (1, 32, 42). Indeed, we also found that, whereas Dex treatment dampened bronchoalveolar cellular infiltration as well as lung Th-2 numbers (not shown) in OVA/alum mice, little to no effect on bronchoalveolar infiltration or lung Th-1, Th-2, and Th-17 numbers (not shown) was seen in OVA/CFA mice. From these features, we conclude that this model is clinically relevant and appears suitable to study communal aspects of the immunopathophysiology of the heterogeneous neutrophilic asthma condition. A previous study, in which OVA-induced airway inflammation was elicited by adoptively transferred Th-2 or Th-17, showed that Th-17 could critically mediate steroid-resistant airway inflammation as well as airway hyperresponsiveness (not assessed in this study) in asthma. This hypothesis is strengthened by the steroid resistance of inflammation in our OVA/CFA model, in which the inflammatory features of neutrophilic and Th-17-dominated asthma may be better represented by the additional Th-1 and Th-2 components. Furthermore, extrapolating to clinical asthma, our results also indicate that eosinophil- versus neutrophil-dominated or steroid-sensitive versus -resistant asthma types may divert already at the stage of allergic sensitization, dictated by the nature of the immune-modulating danger signaling elicited during sensitization.

Comparative analyses of the two models revealed as expected a strong parallel between chemokine expression and cellular composition of the inflammatory response. In the OVA/CFA-model, Th-1-chemoattractants were prominently expressed in contrast with the OVA/alum-model, where Th-2-/eosinophil-recruiting chemokines predominated. However, protein levels of inflammatory mediators in BAL fluid also showed some remarkable resemblances between the models. Thus, IL-1β, IL-6, IL-12p40, CXCL-1, α-chemokines and C3a levels were elevated in both conditions. This observation, along with the notion that there is redundancy in the chemokine and cytokine system (29, 30, 38), could indicate that cytokine measurements in BAL as such may not be adequate to distinguish between the different pathologies. It is nonetheless interesting to point out the significantly higher levels of C3a, IL-1β, IL-6 and especially IFN-γ in the OVA/CFA-mice, since these mediators have been shown to be associated with severe asthma attacks (2, 23, 28, 36, 44). Moreover, IL-17 and MMP-9 expression have been correlated with asthma severity (3, 9, 12, 31). Although IL-17 was markedly increased in the OVA/CFA-model, we found no differences in total and processed MMP-9 in BAL fluid. Also MMP-12 levels and proteolytic activity were strongly increased, in line with a previous report showing a role for MMP-12 in a model of cockroach-induced neutrophil-dominated asthma (48). However, again we found no differences between the models. Thus, although the two experimental models clearly represent different pathologies in terms of cellular inflammation, glucocorticoid sensitivity and Th-cell phenotypes, the inflammatory micro-environment displays a remarkable number of common denominators.

A common constituent in the pulmonary immune cell composition of both eosinophil- and neutrophil-predominant asthma are AM. These long-lived cells are presumed to play pivotal roles

in the orchestration of local inflammation by producing secreted inflammatory mediators and modulating T-cell responses through their antigen-presenting capacities. AM display a remarkable plasticity and can be excellent sensors of the inflammatory micro-environment. Because of these features, their activation state may reflect distinct inflammatory signatures involved in (counter-)acting regulatory checkpoints in neutrophil- or eosinophil-dominated allergic disease. Yet, only fragmented and often contradicting information is available on the precise functions of AM in asthma (24, 39). We therefore performed a genome-wide transcriptome analysis on these cells. A striking first observation was the identification of an important generic inflammatory transcriptional program comprising multiple pro-inflammatory cytokines, chemokines and growth factors, in line with the common pro-inflammatory environment we also observed in the BAL fluid. Genes specifically associated with neutrophilic or eosinophilic inflammatory signatures could mostly be linked with differences in BAL cell composition (Th_1-attracting CXCL9 and CXCL10 in neutrophil- versus Th_2-/eosinophil-recruiting CCL22 and CCL24 in eosinophil-predominant inflammation) or with the earlier mentioned notion that the inflammatory setting in the neutrophil-dominated condition possesses similarities with severe asthma attacks in clinical disease (higher expression of IFN-γ and IL-6).

Importantly, we found indications that AM may also exert subtle immune-modulatory functions. Firstly, we observed a dramatic increase in the mRNA expression of the IL-18 scavenger, IL-18BP, in the neutrophilic severe asthma-like model. Along with a generic down-regulation of IL-18, a cytokine that strongly synergizes with IL-12 and the induction of IL-12b mRNA, this result indicates that in the neutrophil-predominant asthma model IL-12-driven IFN-γ production by Th-1 cells is tightly kept in control. Possibly, an endogenous IFN-γ regulated feedback loop (11)

underlies this regulatory mechanism. It is tempting to speculate that loss of control at the level of the IL-18^{down}/IL-$18BP^{up}$ balance by genetic or environmental factors, resulting in increased IL-18 activity, may contribute to a shift from eosinophil- to neutrophil-predominant asthma and for neutrophil-predominant asthma lead to exacerbation of pathology and lung damage. A second (anti-)inflammatory checkpoint is suggested by the strongly polarized mRNA levels of AM arachidonic acid-metabolizing key-enzymes: in eosinophilic allergic inflammation a pronounced upregulation of *Alox15* and *Ptgs1* is observed as opposed to the increased expression of *Ptgs2* in neutrophil-dominated inflammation. A shift towards LX production through *Alox15* in eosinophilic asthma has been associated with anti-inflammatory activity, as specifically LXA_4 was shown to have beneficial effects in mouse models (4, 7, 27). Conversely, in AM from the neutrophil-dominated inflammation model, a shift towards chiefly prostanoid production is suggested by the increased expression of *Ptgs2*. COX2 (encoded by *Ptgs2*) has a higher affinity for arachidonic acid than COX1 (encoded by *Ptgs1*) (34) and preferentially synthesizes PGE_2 and PGI_2 (8). The role of these two prostanoids in clinical asthma sub-phenotypes is elusive (26), but in the allergically inflamed lung PGE_2 and PGI_2 are considered as anti-inflammatory agents (35, 46). Thus, it appears that there exists a dichotomy in the AM arachidonic acid metabolism by which these cells attempt to control different types of inflammation. Clearly, more studies are required to confirm whether the differential *Ptgs2* versus *Ptgs1/Alox15* pathways in AM could be a discriminative feature of neutrophil versus eosinophil asthma types respectively.

Finally, transcriptome and flowcytometric analyses also provided clues as to how AM may directly modulate local T-cell functions in an antigen-dependent manner. Especially in the neutrophil-predominant condition, an increased capability to exert MHC-I and MHC-II mediated

antigen presentation is apparent; increased expression of genes involved in T-cell communication (*Cd40*), antigen processing (*B2m*, *Tap1*, *Tapbp*, *C2ta*, *H2-Dmb1*, *H2-Dmb2*, *H2-Oa*) and presentation (*H2-M3*, *Qa-1*, *Qa-2*, *Ii*, *H2-Aa*, *H2-Ab1*, *H2-Eb1*) supports this. However, the outcome of antigen recognition by local T-cells may be attenuation rather than activation. Thus, we observed a dominant expression of co-inhibitory (*Cd274* and *Pdcd1lg2*) over co-stimulatory (*Cd80*, *Cd86*, and *Icosl*) ligands. The gene products of *Cd274* and *Pdcd1lg2*, respectively PD-L1 and PD-L2, have been reported to counteract established Th_1- and Th_2-mediated immune responses and to induce immunological tolerance (22, 40). Flowcytometric analysis of AM further supported this proposition. In the neutrophil-predominant condition, MHC-II surface levels were clearly upregulated, indicating enhanced antigen presentation capacities. Likewise, co-inhibitory PD-L1 levels were strongly increased in the total AM population. In contrast, AM from the eosinophilic condition showed only little up-regulation of MHC-II. As expected, DC showed all characteristics of potent APC - strongly increased surface levels of CD40, MHC-II and CD86 – in either model, but again in the neutrophilic model a bias towards T-cell attenuation is indicated by the selective increase of PD-L1.

In conclusion, in this study we established a CFA-based mouse model mimicking the inflammatory and glucocorticoid-resistant component of neutrophil-predominant asthma. Moreover, our results demonstrate the crucial role of immune potentiating factors present during allergic sensitization in determining the nature of the ensuing bronchial allergic response. Furthermore, we identified distinctive endogenous regulatory checkpoints superimposed onto a generic inflammatory environment potentially controlling the observed phenotype. These findings underscore the clinical relevance of comparative studies using the here documented

OVA/CFA-based model of neutrophilic allergic inflammation as a counterpart for the conventional OVA/alum-based model of eosinophilic allergic inflammation. Mechanistic studies addressing the identified anti-inflammatory balances - tight control of IL-12/IL-18 activity, prostanoids-biased arachidonic acid metabolism, and local T-cell attenuation - may lead to new insights and innovative therapeutic approaches to treat neutrophil-dominated asthma types.

Acknowledgements

We like to thank Seppe Vander Beken for technical assistance and Chris Van Hove for help with the manuscript.

Grants

This work was supported by the Research Foundation-Flanders grants G.0376.05N and G.0063.09N, the Inflammatrack project 80016 from the Flanders Institute for Innovation and Technology, and the Ghent University Methusalem BOF09/01M00709 grant. Additional financial support to J.G. and J.P. was provided by the IAP6/18, funded by the Interuniversity Attraction Poles Program and initiated by the Belgian State Science Policy Office.

References

1. **Al-Ramli W, Prefontaine D, Chouiali F, Martin JG, Olivenstein R, Lemiere C, and Hamid Q**. T(H)17-associated cytokines (IL-17A and IL-17F) in severe asthma. *J Allergy Clin Immunol* 123: 1185-1187, 2009.

2. **Ali H, and Panettieri RA, Jr.** Anaphylatoxin C3a receptors in asthma. *Respir Res* 6: 19, 2005.

3. **Atkinson JJ, and Senior RM**. Matrix metalloproteinase-9 in lung remodeling. *Am J Respir Cell Mol Biol* 28: 12-24, 2003.

4. **Barnes PJ**. Endogenous inhibitory mechanisms in asthma. *Am J Respir Crit Care Med* 161: S176-181, 2000.

5. **Barnes PJ**. Immunology of asthma and chronic obstructive pulmonary disease. *Nat Rev Immunol* 8: 183-192, 2008.

6. **Bogaert P, Tournoy KG, Naessens T, and Grooten J**. Where asthma and hypersensitivity pneumonitis meet and differ: noneosinophilic severe asthma. *Am J Pathol* 174: 3-13, 2009.

7. **Bonnans C, Chanez P, and Chavis C**. Lipoxins in asthma: potential therapeutic mediators on bronchial inflammation? *Allergy* 59: 1027-1041, 2004.

8. **Brock TG, McNish RW, and Peters-Golden M**. Arachidonic acid is preferentially metabolized by cyclooxygenase-2 to prostacyclin and prostaglandin E2. *J Biol Chem* 274: 11660-11666, 1999.

9. **Bullens DM, Truyen E, Coteur L, Dilissen E, Hellings PW, Dupont LJ, and Ceuppens JL**. IL-17 mRNA in sputum of asthmatic patients: linking T cell driven inflammation and granulocytic influx? *Respir Res* 7: 135, 2006.

10. **Chanez P, Wenzel SE, Anderson GP, Anto JM, Bel EH, Boulet LP, Brightling CE, Busse WW, Castro M, Dahlen B, Dahlen SE, Fabbri LM, Holgate ST, Humbert M, Gaga M, Joos GF, Levy B, Rabe KF, Sterk PJ, Wilson SJ, and Vachier I**. Severe asthma in adults: what are the important questions? *J Allergy Clin Immunol* 119: 1337-1348, 2007.

11. **Corbaz A, ten Hove T, Herren S, Graber P, Schwartsburd B, Belzer I, Harrison J, Plitz T, Kosco-Vilbois MH, Kim SH, Dinarello CA, Novick D, van Deventer S, and Chvatchko Y**. IL-18-binding protein expression by endothelial cells and macrophages is up-regulated during active Crohn's disease. *J Immunol* 168: 3608-3616, 2002.

12. **Cundall M, Sun Y, Miranda C, Trudeau JB, Barnes S, and Wenzel SE**. Neutrophil-derived matrix metalloproteinase-9 is increased in severe asthma and poorly inhibited by glucocorticoids. *J Allergy Clin Immunol* 112: 1064-1071, 2003.

13. **Douwes J, Gibson P, Pekkanen J, and Pearce N**. Non-eosinophilic asthma: importance and possible mechanisms. *Thorax* 57: 643-648, 2002.

14. **Epstein MM**. Do mouse models of allergic asthma mimic clinical disease? *Int Arch Allergy Immunol* 133: 84-100, 2004.

15. **Fahy JV**. Eosinophilic and neutrophilic inflammation in asthma: insights from clinical studies. *Proc Am Thorac Soc* 6: 256-259, 2009.

16. **Girard M, Lacasse Y, and Cormier Y**. Hypersensitivity pneumonitis. *Allergy* 64: 322-334, 2009.

17. **Hashimoto T, Akiyama K, Kobayashi N, and Mori A**. Comparison of IL-17 production by helper T cells among atopic and nonatopic asthmatics and control subjects. *Int Arch Allergy Immunol* 137 Suppl 1: 51-54, 2005.

18. **Holgate ST**. Pathogenesis of asthma. *Clin Exp Allergy* 38: 872-897, 2008.

19. **Huang da W, Sherman BT, and Lempicki RA**. Systematic and integrative analysis of large gene lists using DAVID bioinformatics resources. *Nat Protoc* 4: 44-57, 2009.

20. **Joshi AD, Fong DJ, Oak SR, Trujillo G, Flaherty KR, Martinez FJ, and Hogaboam CM**. Interleukin-17-mediated immunopathogenesis in experimental hypersensitivity pneumonitis. *Am J Respir Crit Care Med* 179: 705-716, 2009.

21. **Kamath AV, Pavord ID, Ruparelia PR, and Chilvers ER**. Is the neutrophil the key effector cell in severe asthma? *Thorax* 60: 529-530, 2005.

22. **Keir ME, Francisco LM, and Sharpe AH**. PD-1 and its ligands in T-cell immunity. *Curr Opin Immunol* 19: 309-314, 2007.

23. **Krug N, Tschernig T, Erpenbeck VJ, Hohlfeld JM, and Kohl J**. Complement factors C3a and C5a are increased in bronchoalveolar lavage fluid after segmental allergen provocation in subjects with asthma. *Am J Respir Crit Care Med* 164: 1841-1843, 2001.

24. **Lambrecht BN**. Alveolar macrophage in the driver's seat. *Immunity* 24: 366-368, 2006.

25. **Lemiere C, Ernst P, Olivenstein R, Yamauchi Y, Govindaraju K, Ludwig MS, Martin JG, and Hamid Q**. Airway inflammation assessed by invasive and noninvasive means in severe asthma: eosinophilic and noneosinophilic phenotypes. *J Allergy Clin Immunol* 118: 1033-1039, 2006.

26. **Levy BD, Bonnans C, Silverman ES, Palmer LJ, Marigowda G, and Israel E**. Diminished lipoxin biosynthesis in severe asthma. *Am J Respir Crit Care Med* 172: 824-830, 2005.

27. **Levy BD, De Sanctis GT, Devchand PR, Kim E, Ackerman K, Schmidt BA, Szczeklik W, Drazen JM, and Serhan CN**. Multi-pronged inhibition of airway hyper-responsiveness and inflammation by lipoxin A(4). *Nat Med* 8: 1018-1023, 2002.

28. **Linden A**. Role of interleukin-17 and the neutrophil in asthma. *Int Arch Allergy Immunol* 126: 179-184, 2001.

29. **Lloyd CM, and Brown Z**. Chemokine receptors : therapeutic potential in asthma. *Treat Respir Med* 5: 159-166, 2006.

30. **Mantovani A, Sica A, Sozzani S, Allavena P, Vecchi A, and Locati M**. The chemokine system in diverse forms of macrophage activation and polarization. *Trends Immunol* 25: 677-686, 2004.

31. **Mattos W, Lim S, Russell R, Jatakanon A, Chung KF, and Barnes PJ**. Matrix metalloproteinase-9 expression in asthma: effect of asthma severity, allergen challenge, and inhaled corticosteroids. *Chest* 122: 1543-1552, 2002.

32. **McKinley L, Alcorn JF, Peterson A, Dupont RB, Kapadia S, Logar A, Henry A, Irvin CG, Piganelli JD, Ray A, and Kolls JK**. TH17 cells mediate steroid-resistant airway inflammation and airway hyperresponsiveness in mice. *J Immunol* 181: 4089-4097, 2008.

33. **Mohr LC**. Hypersensitivity pneumonitis. *Curr Opin Pulm Med* 10: 401-411, 2004.

34. **Murakami M, Kambe T, Shimbara S, and Kudo I**. Functional coupling between various phospholipase A2s and cyclooxygenases in immediate and delayed prostanoid biosynthetic pathways. *J Biol Chem* 274: 3103-3115, 1999.

35. **Nagao K, Tanaka H, Komai M, Masuda T, Narumiya S, and Nagai H**. Role of prostaglandin I2 in airway remodeling induced by repeated allergen challenge in mice. *Am J Respir Cell Mol Biol* 29: 314-320, 2003.

36. **Nakano Y, Morita S, Kawamoto A, Suda T, Chida K, and Nakamura H**. Elevated complement C3a in plasma from patients with severe acute asthma. *J Allergy Clin Immunol* 112: 525-530, 2003.

37. **Ordonez CL, Shaughnessy TE, Matthay MA, and Fahy JV**. Increased neutrophil numbers and IL-8 levels in airway secretions in acute severe asthma: Clinical and biologic significance. *Am J Respir Crit Care Med* 161: 1185-1190, 2000.

38. **Ozaki K, and Leonard WJ**. Cytokine and cytokine receptor pleiotropy and redundancy. *J Biol Chem* 277: 29355-29358, 2002.

39. **Peters-Golden M**. The alveolar macrophage: the forgotten cell in asthma. *Am J Respir Cell Mol Biol* 31: 3-7, 2004.

40. **Radhakrishnan S, Iijima K, Kobayashi T, Kita H, and Pease LR**. Dendritic cells activated by cross-linking B7-DC (PD-L2) block inflammatory airway disease. *J Allergy Clin Immunol* 116: 668-674, 2005.

41. **Schuyler M, Gott K, and Haley P**. Experimental murine hypersensitivity pneumonitis. *Cell Immunol* 136: 303-317, 1991.

42. **Shannon J, Ernst P, Yamauchi Y, Olivenstein R, Lemiere C, Foley S, Cicora L, Ludwig M, Hamid Q, and Martin JG**. Differences in airway cytokine profile in severe asthma compared to moderate asthma. *Chest* 133: 420-426, 2008.

43. **Simonian PL, Roark CL, Wehrmann F, Lanham AK, Diaz del Valle F, Born WK, O'Brien RL, and Fontenot AP**. Th17-polarized immune response in a murine model of hypersensitivity pneumonitis and lung fibrosis. *J Immunol* 182: 657-665, 2009.

44. **Tillie-Leblond I, Gosset P, and Tonnel AB**. Inflammatory events in severe acute asthma. *Allergy* 60: 23-29, 2005.

45. **van Rijt LS, Kuipers H, Vos N, Hijdra D, Hoogsteden HC, and Lambrecht BN**. A rapid flow cytometric method for determining the cellular composition of bronchoalveolar lavage fluid cells in mouse models of asthma. *J Immunol Methods* 288: 111-121, 2004.

46. **Vancheri C, Mastruzzo C, Sortino MA, and Crimi N**. The lung as a privileged site for the beneficial actions of PGE2. *Trends Immunol* 25: 40-46, 2004.

47. **Vermaelen K, and Pauwels R**. Accurate and simple discrimination of mouse pulmonary dendritic cell and macrophage populations by flow cytometry: methodology and new insights. *Cytometry A* 61: 170-177, 2004.

48. **Warner RL, Lukacs NW, Shapiro SD, Bhagarvathula N, Nerusu KC, Varani J, and Johnson KJ**. Role of metalloelastase in a model of allergic lung responses induced by cockroach allergen. *Am J Pathol* 165: 1921-1930, 2004.

49. **Yi ES**. Hypersensitivity pneumonitis. *Crit Rev Clin Lab Sci* 39: 581-629, 2002.

Legends to the figures

Figure 1. Characterization of pulmonary immune cell populations in mice exposed to OVA aerosols after systemic sensitization against OVA in the presence of either CFA (OVA/CFA) or alum (OVA/alum), and control (naïve) mice (n=6). (A) Average BAL cell count ± SE. (B) Average BAL cellular composition ± SE, determined by flowcytometric enumeration of eosinophils (CD3ε/B220$^-$ I-Ab$^-$ CD11c$^-$ CCR3$^+$ SSC^{hi}), neutrophils (CD3ε/B220$^-$ I-Ab$^-$ CD11c$^-$ CCR3$^-$ SSC^{med}), AM (CD3ε/B220$^-$ I-Ab$^{med/hi}$ CD11c$^+$ autofluo^{hi}), DC (CD3ε/B220$^-$ I-Ab^{hi} CD11c$^+$ autofluo^{lo}) and lymphocytes (CD3ε/B220$^+$ CD11c$^-$). (C) Microscopic evaluation of pulmonary inflammation in peribronchiolar and interstitial regions on H&E stained sections of lavaged lungs. *: $p<0.05$, **: $p<0.01$, ***: $p<0.001$, N.S.: not significant.

Figure 2. Characterization of BAL immune cell populations in (A) OVA/alum and (B) OVA/CFA mice, treated with 0, 1, or 2.5mg/kg of Dex (i.p.) 3h prior to OVA challenge (n=7/group). Average BAL cellular composition ± SE, determined by flowcytometric analysis of eosinophils (CD3ε$^-$ I-Ab$^-$ CD11c$^-$ CD11b^{med} CCR3$^+$ SSC^{hi}), neutrophils (CD3ε$^-$ I-Ab$^-$ CD11c$^-$ CD11b^{hi} CCR3$^-$ SSC^{med}), resident AM (CD3ε$^-$ I-Ab$^{med/hi}$ CD11b^{lo} CD11c$^+$ autofluo^{hi}), recruited AM (CD3ε$^-$ I-Ab$^{med/hi}$ CD11b$^+$ CD11c$^+$ autofluo^{med}), DC (CD3ε$^-$ I-Ab^{hi} CD11c$^+$ autofluo^{lo}) and CD4 T-cells (CD3ε$^+$ CD4$^+$ CD11c$^-$). *: $p<0.05$, **: $p<0.01$, ***: $p<0.001$, N.S.: not significant. Gating strategy is provided in Suppl. Fig. 2A.

Figure 3. Characterization of local pulmonary T-cell populations in OVA/CFA, OVA/alum and naïve mice. (A) Relative mRNA expression levels ± SD of Th-1 (*T-bet*), Th-2 (*Gata3*), and Th-17 (*Rorgt*) associated transcription factors in purified pulmonary CD4 T-cells, pooled from 5

(OVA/CFA, OVA/alum) or 10 (naïve) mice/group. (B) Average levels ± SD of pulmonary Th populations in lung leukocytes (pooled from 6 mice/group) after *in vitro* α-CD3 re-activation, determined by flowcytometric analysis of Th-1 ($CD45^+$ $CD4^+$ I-Ab/F4/80^- $IL\text{-}17^-$ IFN-γ^+), Th-2 ($CD45^+$ $CD4^+$ I-Ab/F4/80^- $IL\text{-}4^+$) and Th-17 ($CD45^+$ $CD4^+$ I-Ab/F4/80^- $IL\text{-}17^+$). Gating strategy is provided in Suppl. Fig. 2B. (C) Average BAL fluid levels of T-cell associated cytokines ± SE (n=4/group). *: $p<0.05$, **: $p<0.01$, ***: $p<0.001$, N.S.: not significant.

Figure 4. Characterization of local innate inflammatory mediator signatures in naïve, OVA/CFA and OVA/alum mice. (A) mRNA expression levels ± SD of Th-1-recruiting (*Cxcl9*, *Cxcl10*) and Th_2/eosinophil-recruiting (*Ccl9*, *Ccl11*) chemokines in lungs, pooled from 5 mice/group. (B) Average BAL fluid levels ± SE of inflammatory cytokines and chemokines (n=4/group). (C) Average BAL fluid levels ± SE of total and active MMP-9 and MMP-12 (n=5) and (D) complement C3a (n=5). *: $p<0.05$, **: $p<0.01$, ***: $p<0.001$, N.S.: not significant.

Figure 5. Identification of common and condition-specific over- and underrepresented biological themes in the AM transcriptome by genome-wide transcriptome profiling of pooled AM, isolated from 10 (OVA/CFA, OVA/alum) or 15 (naïve) mice/group. Transcripts, more than 2-fold differentially expressed in OVA/CFA and/or OVA/alum versus naïve condition were withheld for unbiased *in silico* functional clustering analysis. Shown are n-fold enrichment of genes within each biological theme, and its p-value (Expression Analysis Systematic Explorer or EASE score). EASE < 1.10^{-4} was considered significantly over- or underrepresented.

Figure 6. Selection of generic, condition-biased and condition-specific genes from the genome-wide transcriptome data set. Selected genes comprise (A) chemokines, (B) cytokines and growth factors, (C) arachidonic acid metabolites, and (D) genes involved in antigen processing and presentation. Shown are scatter plots of gene transcript expression ratios in either OVA/CFA condition vs. naïve (Y-axis) or OVA/alum condition vs. naïve (X-axis), and their classification into 'generic' (≤ 2-fold differences between OVA/CFA and OVA/alum vs. naïve), 'condition-biased' (> 2- and ≤ 5-fold differences between OVA/CFA and OVA/alum vs. naïve) or 'condition-specific' (> 5-fold differences between OVA/CFA and OVA/alum vs. naïve) signatures. √ indicates the induction levels of genes which were tested and confirmed by RT-qPCR in a biologically independent repeat experiment.

Figure 7. Surface expression of AM and DC ligands involved in antigen presentation and T-cell interaction. (A) Flowcytometric discrimination of AM and DC based on autofluorescence and surface expression of CD11c. Gating strategy was based on *Vermaelen et al.*, *Cytometry, 2004* (43). (B-G) Flowcytometric analysis of co-stimulatory surface markers on AM and DC from OVA/CFA and OVA/alum vs. naïve condition (gated within high autofluorescent/$CD11c^+$ cell populations for AM and low autofluorescent/$CD11c^+$ cell populations for the DC). Results were obtained by analyzing pooled BAL cells from 8 mice/group. Data shown are representative of 2 biologically independent experiments. (B) n-fold induction levels of median fluorescence intensities. (C-G) Surface expression of CD40, CD80, CD86, PD-L1 and PD-L2 in relation to MHC-II expression on AM and DC in the 3 conditions.

Suppl Figure 1. PCR Primers, used in this manuscript

Suppl Figure 2. Flowcytometric gating strategies, used in this manuscript. (A) BAL immune cell phenotyping based on cellular autofluorescence, side scatter and surface expression of CD3ε, CD4, MHCII (I-Ab), CD11c, CD11b and CCR3. Eosinophils are $CD3\varepsilon^-$ $I\text{-}Ab^-$ $CD11c^-$ $CD11b^{med}$ $CCR3^+$ SSC^{hi}, neutrophils are $CD3\varepsilon^-$ $I\text{-}Ab^-$ $CD11c^-$ $CD11b^{hi}$ $CCR3^-$ SSC^{med}, resident AM are $CD3\varepsilon^-$ $I\text{-}Ab^{med/hi}$ $CD11b^{lo}$ $CD11c^+$ $autofluo^{hi}$, recruited AM are $CD3\varepsilon^-$ $I\text{-}Ab^{med/hi}$ $CD11b^+$ $CD11c^+$ $autofluo^{med}$, DC are $CD3\varepsilon^-$ $I\text{-}Ab^{hi}$ $CD11c^+$ $autofluo^{lo}$ and CD4 T-cells are $CD3\varepsilon^+$ $CD4^+$ $CD11c^-$. Note: Some $CD11c^+$ cells in this Figure appear false positive for CD3ε because of autofluorescence in the CD3ε channel (FITC). (B) Pulmonary Th-1/Th-2/Th-17 phenotyping based on surface expression of CD45, CD4, MHC-II (I-Ab), F4/80, and intracellular expression of IL-17, IFN-γ, and IL-4. Lung leukocytes were identified as $CD45^+$, and a dump channel for $I\text{-}Ab^+$ or $F4/80^+$ cells was used to get rid of B cells, DC and AM. CD4 T-cells were thus identified as $CD45^+$ $CD4^+$ $I\text{-}Ab/F4/80^-$. IL-17 positivity was used first to identify Th-17 because these cells may also express IFN-γ. Th-1 and Th-2 were then identified as $IL\text{-}17^-$ $IL\text{-}4^-$ $IFN\text{-}\gamma^+$ resp. $IL\text{-}17^-$ $IL\text{-}4^+$ $IFN\text{-}\gamma^-$. Positivity for intracellular cytokines was defined as signal above isotype control.

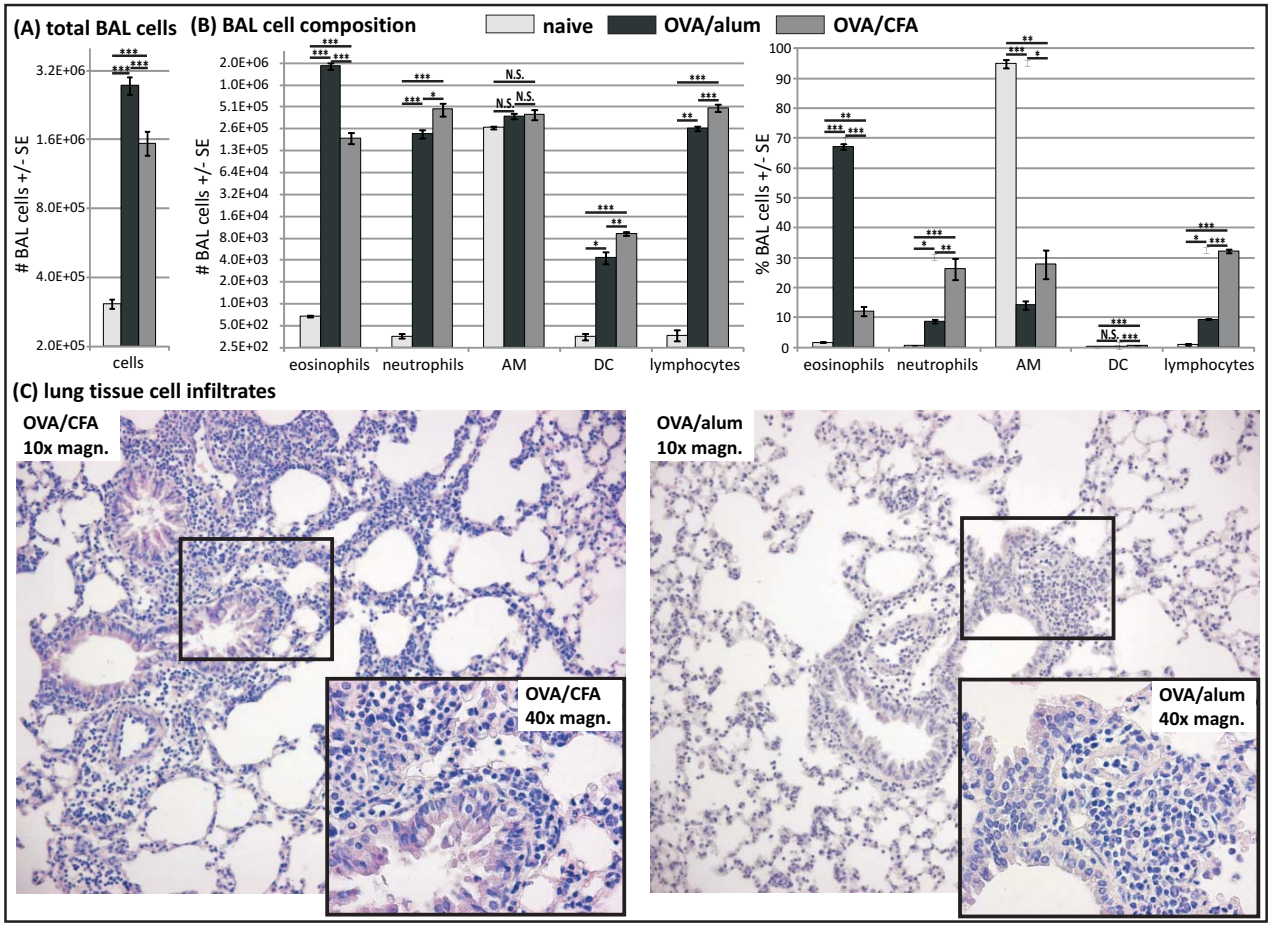
(A) total BAL cells
(B) BAL cell composition
naive
OVA/alum
OVA/CFA
BAL cells +/- SE
cells
eosinophils
neutrophils
AM
DC
lymphocytes
% BAL cells +/- SE
(C) lung tissue cell infiltrates
OVA/CFA
10x magn.
OVA/CFA
40x magn.
OVA/alum
10x magn.
OVA/alum
40x magn.

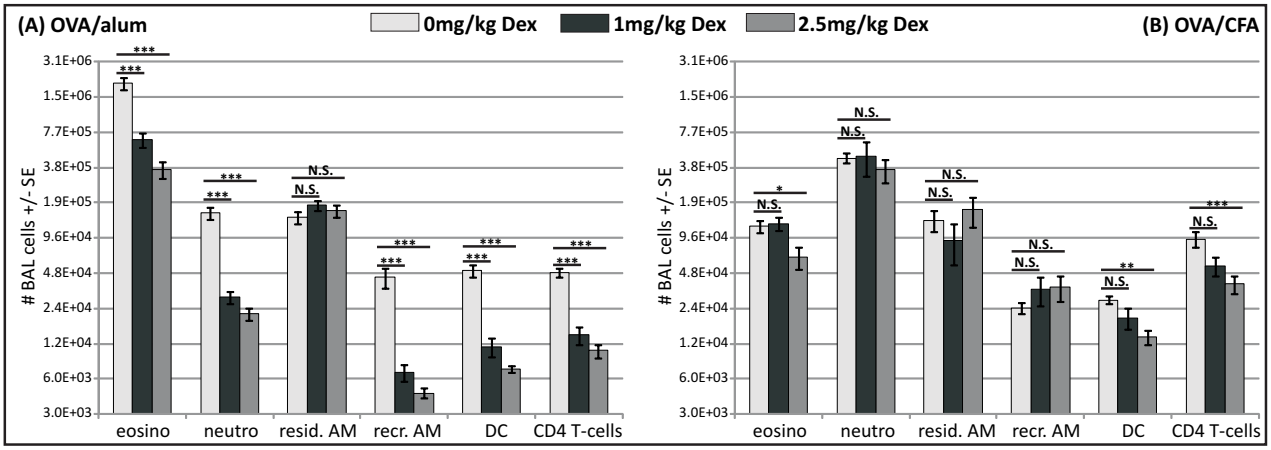
(A) OVA/alum
0mg/kg Dex
1mg/kg Dex
2.5mg/kg Dex
(B) OVA/CFA
BAL cells +/- SE
3.1E+06
1.5E+06
7.7E+05
3.8E+05
1.9E+05
9.6E+04
4.8E+04
2.4E+04
1.2E+04
6.0E+03
3.0E+03
eosino
neutro
resid. AM
recr. AM
DC
CD4 T-cells
***
**
*
N.S.

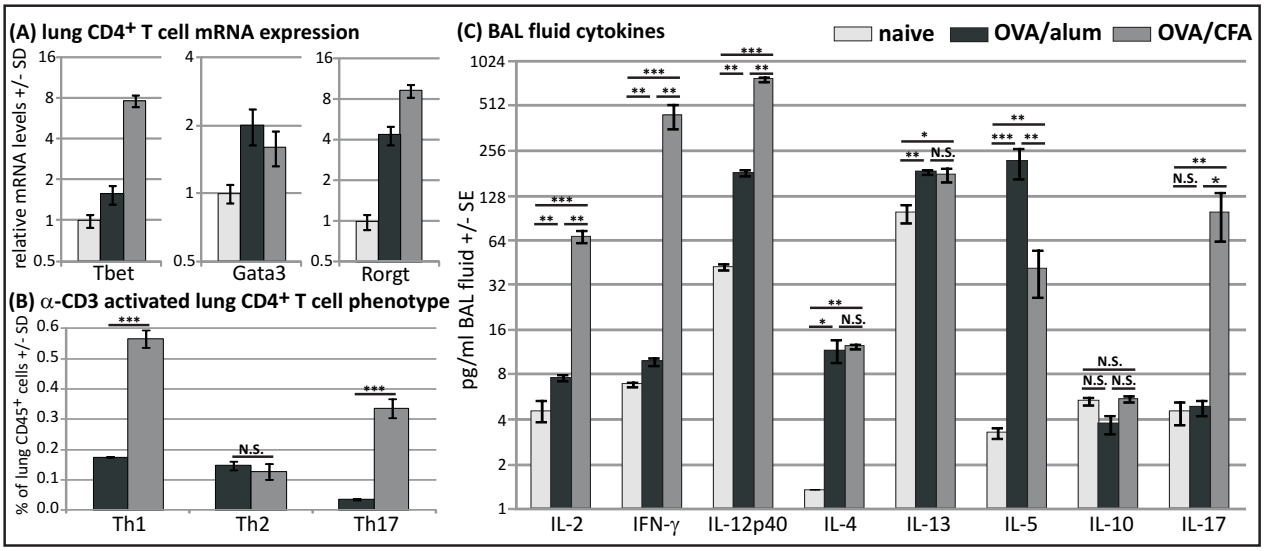
(A) lung CD4+ T cell mRNA expression
relative mRNA levels +/- SD
Tbet
Gata3
Rorgt
(B) α-CD3 activated lung CD4+ T cell phenotype
% of lung CD45+ cells +/- SD
Th1
Th2
Th17
N.S.
(C) BAL fluid cytokines
naive
OVA/alum
OVA/CFA
pg/ml BAL fluid +/- SE
IL-2
IFN-γ
IL-12p40
IL-4
IL-13
IL-5
IL-10
IL-17

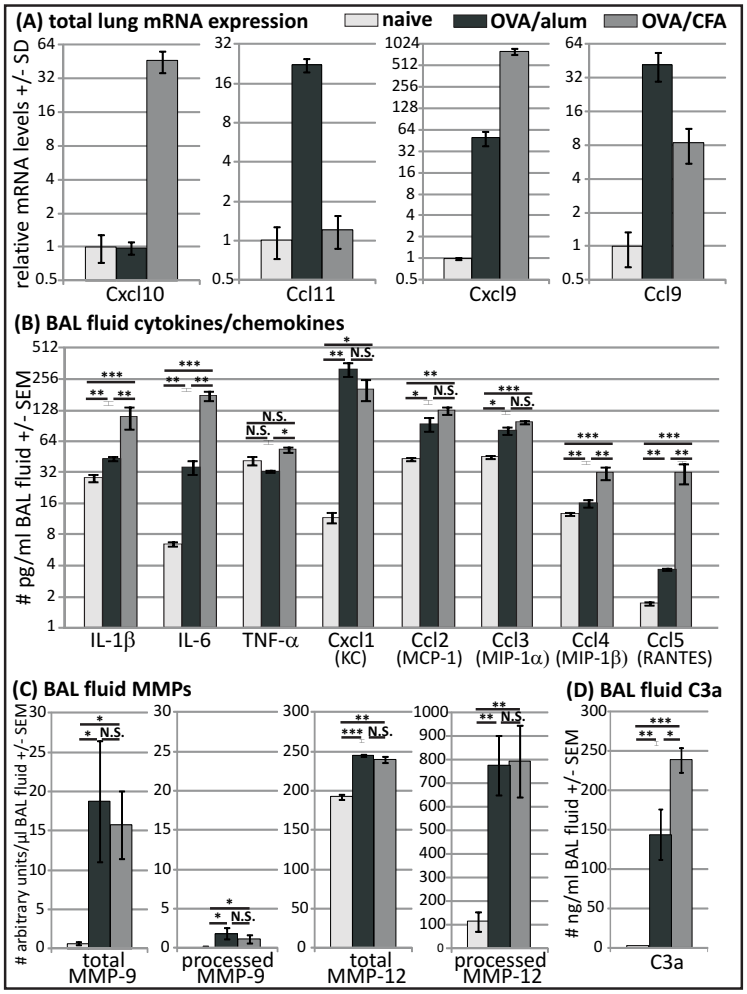
(A) total lung mRNA expression
naive
OVA/alum
OVA/CFA
relative mRNA levels +/- SD
Cxcl10
Ccl11
Cxcl9
Ccl9
(B) BAL fluid cytokines/chemokines
pg/ml BAL fluid +/- SEM
IL-1β
IL-6
TNF-α
Cxcl1 (KC)
Ccl2 (MCP-1)
Ccl3 (MIP-1α)
Ccl4 (MIP-1β)
Ccl5 (RANTES)
(C) BAL fluid MMPs
arbitrary units/µl BAL fluid +/- SEM
total MMP-9
processed MMP-9
total MMP-12
processed MMP-12
(D) BAL fluid C3a
ng/ml BAL fluid +/- SEM
C3a
N.S.

GENES, MORE THAN 2-FOLD UPREGULATED COMPARED TO NAIVE CONDITION							
		COMMON (1508 genes)		UNIQUE OVA/CFA (836 genes)		UNIQUE OVA/alum (970 genes)	
CATEGORY	TERM	N-FOLD ENRICHMENT	P-VALUE (EASE)	N-FOLD ENRICHMENT	P-VALUE (EASE)	N-FOLD ENRICHMENT	P-VALUE (EASE)
KEGG	Cytokine-cytokine receptor interaction	2.49	2.99E-10	2.28	4.45E-5		
SP_PIR	Inflammatory response	4.74	2.24E-9				
SP_PIR	Inflammation	9.77	2.86E-9				
SP_PIR	Cytokine	2.83	1.45E-7	3.40	3.02E-7		
SP_PIR	Chemotaxis	4.55	1.78E-7				
SP_PIR	Phosphoprotein	1.26	2.23E-7				
KEGG	Antigen processing and presentation	3.35	2.35E-7	6.07	1.17E-13		
SP_PIR	Transmembrane protein	2.07	3.48E-7				
KEGG	Type I diabetes mellitus	3.77	4.33E-7	4.41	9.75E-6		
SP_PIR	Alternative splicing	1.28	1.01E-6	1.27	2.54E-4		
KEGG	Cell adhesion molecules	2.51	2.74E-6				
SP_PIR	Heterodimer	4.36	1.01E-5				
SP_PIR	Mhc ii	10.35	1.64E-5				
SP_PIR	Direct protein sequencing	1.47	2.37E-5				
SP_PIR	Immune response	2.62	2.41E-5	3.65	5.42E-7		
KEGG	Hematopoietic cell lineage	2.77	3.70E-5				
KEGG	Jak-STAT signaling pathway	2.18	9.15E-5	2.51	2.81E-4		
SP_PIR	SH3 domain	2.20	1.18E-4				
SP_PIR	Immunoglobulin domain	1.82	1.66E-4			2.01	1.78E-4
KEGG	Toll-like receptor signaling pathway	2.42	1.86E-4	3.49	4.79E-6		
KEGG	Ubiquitin mediated proteolysis	2.23	2.20E-4				
KEGG	T cell receptor signaling pathway	2.42	2.70E-4			2.75	5.36E-4
SP_PIR	Cytoplasm	1.24	8.60E-4				
KEGG	Natural killer cell mediated cytotoxicity			4.45	6.16E-12		
SP_PIR	Antiviral defense			12.02	2.67E-12		
KEGG	Regulation of autophagy			7.45	2.00E-7		
SP_PIR	Hydrolase			1.64	2.10E-6		
SP_PIR	Apoptosis			2.21	4.21E-4		
SP_PIR	Proteasome			4.39	3.82E-4		
SP_PIR	Innate immunity			4.65	2.42E-4		
SP_PIR	Protease			1.92	1.48E-4		
SP_PIR	Allosteric enzyme			6.89	1.09E-4		
SP_PIR	Heterotetramer					5.12	2.80E-4
SP_PIR	Ubl conjugation					2.09	1.94E-4
GENES, MORE THAN 2-FOLD DOWNREGULATED COMPARED TO NAIVE CONDITION							
		COMMON (632 genes)		UNIQUE OVA/CFA (458 genes)		UNIQUE OVA/alum (575 genes)	
CATEGORY	TERM	N-FOLD ENRICHMENT	P-VALUE (EASE)	N-FOLD ENRICHMENT	P-VALUE (EASE)	N-FOLD ENRICHMENT	P-VALUE (EASE)
SP_PIR	Membrane	1.25	1.48E-5				
KEGG	Pentose and glucuronate interconversions	9.06	1.45E-5	11.68	2.64E-6		
KEGG	Androgen and estrogen metabolism	4.39	7.95E-4	5.67	1.39E-4		
KEGG	Starch and sucrose metabolism	4.02	6.75E-4				
SP_PIR	Transmembrane	1.27	6.10E-4				
SP_PIR	Phosphoprotein			1.41	2.29E-6	1.33	6.27E-6
SP_PIR	Fatty acid metabolism			6.07	9.48E-4		
KEGG	Porphyrin and chlorophyll metabolism			6.25	7.02E-4		
SP_PIR	Cell cycle					2.42	2.78E-5

(A) chemokine mRNA expression

GENE	GENE PRODUCT	Q-PCR CONFIRM
Chemokine (C-C motif) ligand		
Ccl2	MCP-1	✓
Ccl3	MIP-1α	✓
Ccl4	MIP-1β	
Ccl5	RANTES	
Ccl7	MCP-3	
Ccl8	MCP-2	
Ccl9	MIP-1γ	✓
Ccl12	MCP-5	
Ccl17	TARC	
Ccl22	MDC	
Ccl24	Eotaxin-2	✓
Chemokine (C-X-C motif) ligand		
Cxcl1	KC: GROα	
Cxcl2	MIP-2; GROβ	
Cxcl4	PF4	
Cxcl7	NAP2	
Cxcl9	MIG	✓
Cxcl10	IP-10	✓
Cxcl14	MIP-2γ	
Cxcl16	SR-PSOX	

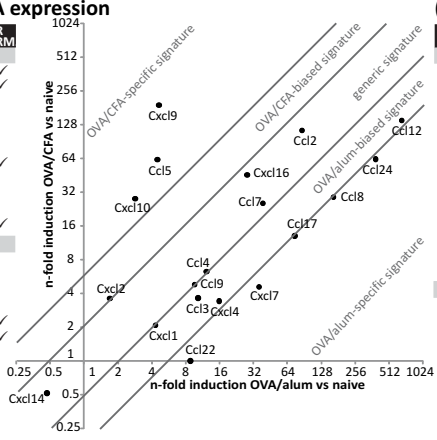

(B) cytokine & growth factor mRNA expression

GENE	GENE PRODUCT	Q-PCR CONFIRM
Cytokines		
Il1a	IL-1α	
Il1b	IL-1β	
Il6	IL-6	✓
Il12b	IL-12p40	✓
Il16	IL-16	
Il18	IL-18	✓
Il18bp	IL-18 binding protein	✓
Ifng	IFN-γ	✓
Ltb	Lymphotoxin-β	
Tnf	TNF-α	✓
Tnfsf9	4-1BB ligand	
Tnfsf10	TRAIL	
Tnfsf13b	TALL-1	
Tnfsf14	LIGHT	
Growth factors		
Csf1	M-CSF	
Gdf15	MIC-1	
Igf1	Insulin-like growth factor 1	
Kitl	Kit ligand	
Pdgfa	PDGF-α	
Pdgfc	PDGF-C	
Tgfb2	TGF-β2	

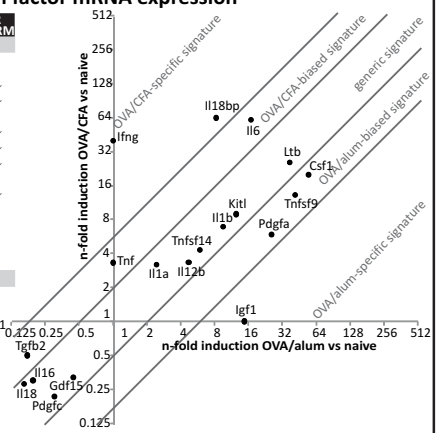

(C) arachidonic acid metabolizing enzyme mRNA expression

GENE	GENE PRODUCT	Q-PCR CONFIRM
Arachidonic acid-metabolizing		
Alox15	12-LOX; 15-lipoxygenase	✓
Alox5	5-LOX; 5-lipoxygenase	✓
Aloxe3	e-LOX-3; Lipoxygenase 3	
Lta4h	Leukotriene A4 hydrolase	
Ltc4s	Leukotriene C4 synthase	✓
Ptgs1	COX1: cyclooxygenase 1	✓
Ptgs2	COX1: cyclooxygenase 1	✓

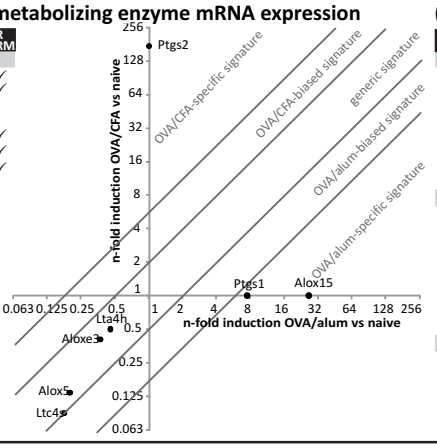

(D) antigen processing & presentation molecule mRNA expression

GENE	GENE PRODUCT	Q-PCR CONFIRM
MHC Class I antigen presentation		
B2m	β-2 microglobulin	
Tap1	TAP; MDR/TAP	
Tapbp	tapasin; TAP binding protein	
H2-K1	H2-K (murine HLA-A1)	
H2-M3	Hmt (murine HLA-F)	
Qa-1	H2-T23 (murine HLA-E)	
Qa-2	H2-Q8 (murine HLA-G)	
MHC Class II antigen presentation		
C2ta	Class II transactivator	
Ii	Ia-γ; CLIP; CD74	
H2-Aa	I-Aα; Ia-1 (murine HLA-DQα1)	
H2-Ab1	I-Aβ; Ia-2 (murine HLA-DQβ1)	
H2-Eb1	I-Eβ; Ia-4 (murine HLA-C)	
H2-Dmb1	H2-Mβ1 (murine HLA-DMβ)	
H2-Dmb2	H2-Mβ2 (murine HLA-DMβ)	
H2-Oa	H2-Oα (murine HLA-DOα)	
T cell interaction and costimulation		
Icam1	CD54	
Cd40	CD40 antigen; Tnfrsf5	
Cd86	CD86 antigen; B7-2	✓
Icosl	ICOS ligand; B7-H2	
Cd274	PD-L1; B7-H1	✓(*)
Pdcd1lg2	PD-L2; B7-DC	✓

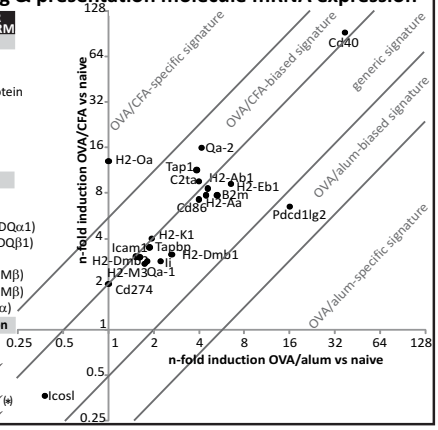

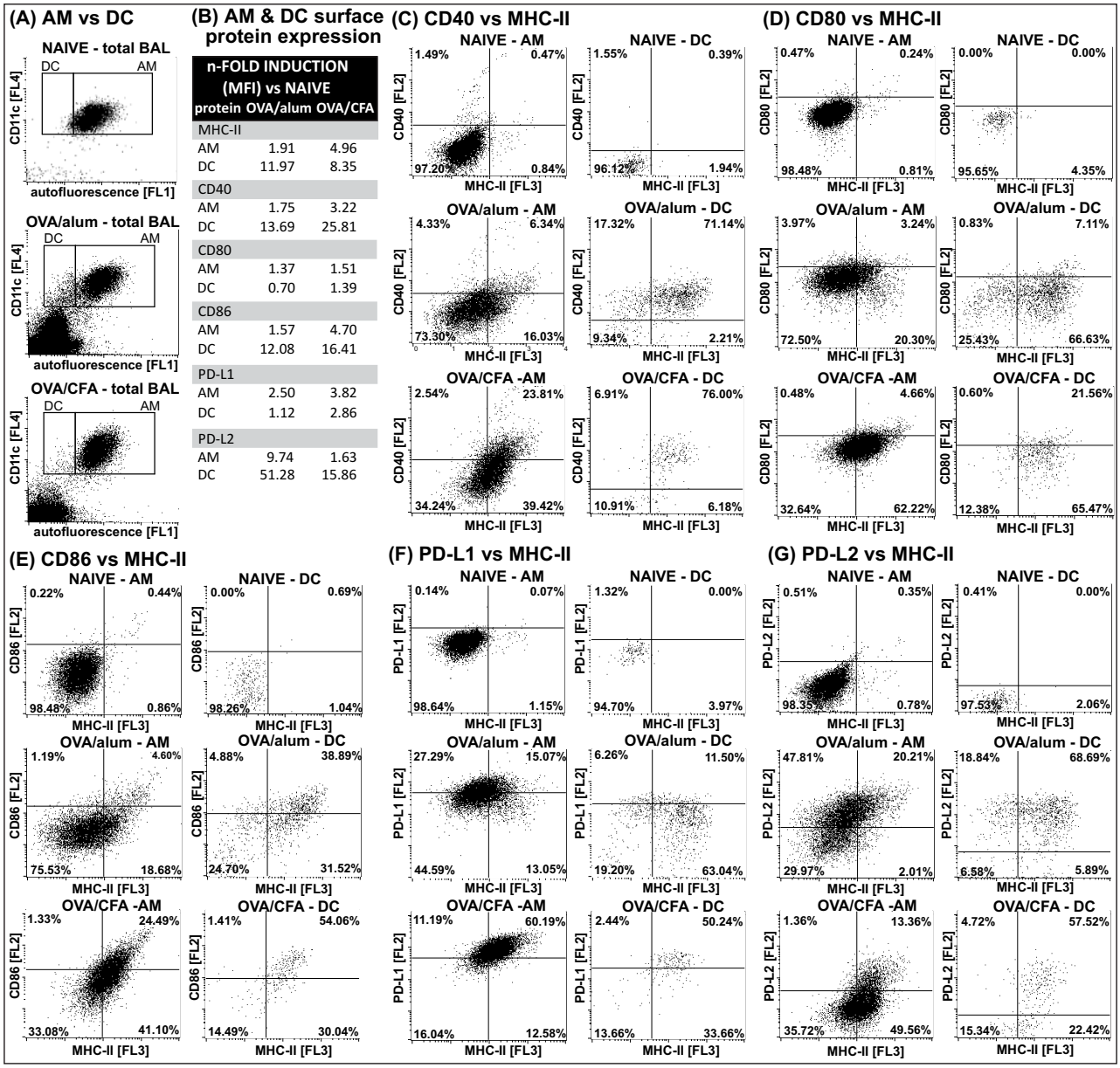
(A) AM vs DC
NAIVE - total BAL
OVA/alum - total BAL
OVA/CFA - total BAL
DC
AM
CD11c [FL4]
autofluorescence [FL1]
(B) AM & DC surface protein expression
n-FOLD INDUCTION (MFI) vs NAIVE
protein OVA/alum OVA/CFA
MHC-II
AM 1.91 4.96
DC 11.97 8.35
CD40
AM 1.75 3.22
DC 13.69 25.81
CD80
AM 1.37 1.51
DC 0.70 1.39
CD86
AM 1.57 4.70
DC 12.08 16.41
PD-L1
AM 2.50 3.82
DC 1.12 2.86
PD-L2
AM 9.74 1.63
DC 51.28 15.86
(C) CD40 vs MHC-II
(D) CD80 vs MHC-II
(E) CD86 vs MHC-II
(F) PD-L1 vs MHC-II
(G) PD-L2 vs MHC-II
NAIVE - AM
NAIVE - DC
OVA/alum - AM
OVA/alum - DC
OVA/CFA -AM
OVA/CFA - DC
MHC-II [FL3]
CD40 [FL2]
CD80 [FL2]
CD86 [FL2]
PD-L1 [FL2]
PD-L2 [FL2]